Structural and electrical properties of $(Ba_{1-x}Sr_x)(Zr_{0.9}M_{0.1})O_3$, M = Y, La, solid solutions

Mirosław M. Bućko [a,*], Magdalena Dudek [b]

[a] AGH University of Science and Technology, Faculty of Materials Science and Ceramics, al. Mickiewicza 30, 30-059 Krakow, Poland
[b] AGH University of Science and Technology, Faculty of Fuel and Energy, Poland

ARTICLE INFO

ABSTRACT

The aim of the work was to study the structural and electrical properties of the $(Ba_{1-x}Sr_x)(Zr_{0.9}Y_{0.1})O_3$ and $(Ba_{1-x}Sr_x)(Zr_{0.9}Y_{0.1})O_3$ solid solutions. The powders of different strontium content ($x = 0$, 0.03, 0.05 and 0.1) were prepared by a thermal decomposition of organo-metallic precursors containing ethylenediaminetetraacetate acid. Some parameters describing stability and transport properties of the perovskite structure, such as tolerance factor, specific free volume and global instability index, were calculated. It was found that the introduction of strontium into both solid solutions caused the increase of specific free volume and global instability index—these structures became a little less stable but, on the other hand, better ionic conductor. All samples were cubic perovskite and the substitution of strontium for barium caused the decrease of respective lattice parameters. Electrical conductivity measurements were performed by the d.c. four-probe method in controlled gas atmospheres containing Ar, air, H_2 and/or H_2O at the temperature from 300 to 800 °C. It was found that the conductivity depended on a chemical composition of the samples and the atmosphere. In general, the electrical conductivity was higher in wet atmospheres which contained oxygen, being in accordance with the model of a proton transport in the perovskite structure which assumed the presence of the oxygen vacancy. The solid solution containing 5 mol.% of strontium showed the highest conductivity and the lowest activation energy of conductivity regardless of the atmospheres.

1. Introduction

There is a growing interest of $MZrO_3$-based materials, where M = Ba, Sr, due to its possible applications as protonic conducting membranes in electrochemical devices such as hydrogen pumps, gas sensors, steam electrolysers, solid oxide fuel cells (SOFC), separators or reactors [1–4]. In general, the $BaZr_{1-x}Y_xO_3$ or $SrZr_{1-x}Y_xO_3$ materials exhibited lower electrical conductivity as compared to $BaCe_{1-x}Y_xO_3$ or $SrCe_{0.9}Y_{0.1}O_3$, respectively, where: $0 < x < 0.2$. However, the chemical and mechanical stability of solid electrolytes involving yttria-doped barium or strontium cerates could be limited in the gas atmospheres involving CO_2, SO_2 and moisture [5,6]. To improve the protonic conductivity of the zirconate materials, a structural modification can be performed. The model of proton migration in perovskites assumes the existence of the two equivalent sites for the proton between the adjacent oxygens in the B-sites, one of which can be occupied by the proton. It reveals the hopping mechanism of the proton changing O–H bond one after another and a distortion of the two neighboring BO_6 octahedrons is necessary

to make this process possible [7,8]. It was stated that proton conductivity in perovskite-type oxides is strictly connected with the differences between radii of the host and dopant ions and their electric charges and the amount of respective dopants [9–11]. There are many studies on the proton conductivity of barium zirconate solid solutions in which the B-site is modified, whereas the studies on the modification of the A-site are rather limited. Our previous work [12] proved that the introduction of 5 mol.% of calcium into barium zirconate solid solution, regardless of atmosphere, leads to the improvement of electrical conductivity compared to $Ba(Y_{0.1}Zr_{0.9})O_3$ sample.

This study is focused on structural and electrical properties of the $(Ba_{1-x}Sr_x)(Zr_{0.9}Y_{0.1})O_3$ and $(Ba_{1-x}Sr_x)(Zr_{0.9}La_{0.1})O_3$ solid solutions as proton conductors.

2. Experimental

All powders were prepared by means of the polymer complex method with the use of versenate acid (ethylenediaminetetraacetate acid—EDTA). The starting aqueous solutions were prepared by dissolving appropriate amounts of barium, strontium, zirconyl, yttrium or lanthanum nitrates (Merck, p.a.) in distilled water. However, as versenate acid's solubility in water is very poor, it was

* Corresponding author. Tel.: +48 12 617 35 72; fax: +48 12 617 24 93.
E-mail address: bucko@agh.edu.pl (M.M. Bućko).

dissolved in a concentrate solution of ammonia. The ammonium versenate solution was added dropwise into a vigorously agitated solution of the respective cation nitrates. During this operation some increase of turbidity was observed due to hydrolysis of the versenate acid. By fixing pH values at about 8 with concentrated ammonia, it led to dissipation of this turbidity. The amount (in moles) of introduced ammonium versenate exceeded by 10% of the total amount of cation moles. The solutions, after being stored for 24 h at room temperature, were dried at 250 °C. The solutions changed their tint while drying, from colourless through yellow to dark-brown, and at this stage a dense, viscous liquid was obtained (resin). By further drying it, this led to a disintegration of this resin, releasing significant amounts of gases and finally setting into a very porous and black solid body. The total drying time extended 12 h. The prepared precursors were initially calcined at 600 °C for 2 h in order to completely remove carbon and/or the rest of organic phases, and then at 1200 °C for 2 h. The powders were ground in the rotary-vibratory mill in dry isopropyl alcohol for 2 h using zirconia grinding media. Isostatic pressing at 250 MPa was used to compact the powders which were then sintered at 1600 °C for 2 h. The procedure described above allowed us to prepare samples with the following chemical composition $(Ba_{1−x}Sr_x)(Zr_{0.9}Y_x)O_3$, where $x = 0$, 0.03, 0.05 and 0.1. The samples are described in the text as B-ZY, B03S-ZY, B05S-ZY and B10S-ZY, respectively. The second sample series was $(Ba_{1−x}Sr_x)Zr_{0.9}La_{0.1}O_3$, where $x = 0$, 0.05, 0.1, which were mentioned in the text as B-ZL, B05S-ZL and B10S-ZL, respectively.

Some structural parameters, such as Goldsmith tolerance factor, t, specific free volume, SFV and global instability index, GII, describing the perovskite structure, were calculated using the SPuDS software package [13]. The phase composition of all powders and sintered bodies were identified by the X-ray diffraction analysis based on ICDD data base. XRD measurements were done using Panalytical X'Pert Pro system with monochromatic Cu K$_\alpha$ radiation. Lattice parameters of the identified phases were determined using the Rietveld refinement method.

The oxygen ion transference numbers of all samples were estimated from electromotive force (emf) measurements of the solid oxide galvanic cell:

$$Pt|Cu, Cu_2O|(Ba_{1−x}Sr_x)(Zr_{0.9}M_{0.1})O_3|Ni, NiO|Pt$$
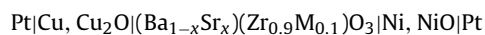
where M = Y or La   (1)

The two-phase mixtures (Cu, Cu$_2$O) and (Ni, NiO) with the known equilibrium oxygen partial pressures were used to provide fixed oxygen potentials at the electrodes [14]. The procedure was practically the same as of that presented in the work of Kiukola and Wagner concerning solid oxide galvanic cells involving the cubic phase of the CaO–ZrO$_2$ solid solution [15]. The ionic transference numbers (t_{ion}) of the samples were determined basing on the emf values, (E_m) measured for the cell (1) and on the emf values (E_t), obtained for the same cell with a pure oxygen ion conductor, Ca$_{0.13}$Zr$_{0.87}$O$_2$ (13CSZ), as an electrolyte:

$$t_{ion} = \frac{E_m}{E}$$ (2)

The total electrical conductivity was measured by the d.c. four-probe method in the temperature range 300–800 °C in different gas atmospheres, such as synthetic air, argon and mixtures of 2 vol.% H$_2$ in Ar. These gases were dry or saturated with water vapour using the water bubbler (RH = 100% at 25 °C). Prior to electrical measurements the Pt electrodes (Heraus) were applied at respective places of the rectangular samples.

3. Results and discussion

Tolerance factor, t, and specific free volume, SFV, are important structural parameters determining stability and symmetry of the
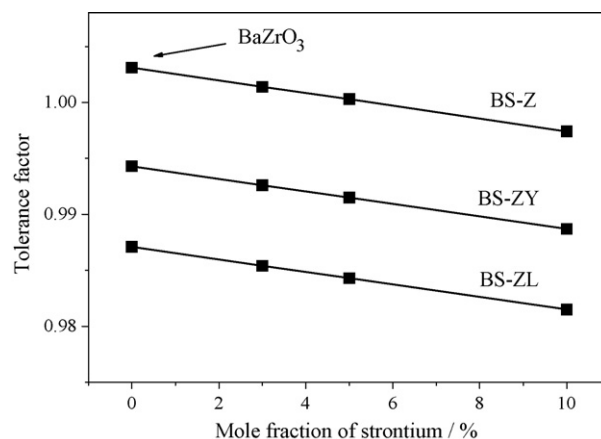

Fig. 1. Compositional dependence of the tolerance factor for $(Ba_{1−x}Sr_x)(Zr_{0.9}M_{0.1})O_3$, M = Y, La, solid solutions.

perovskite structure as well as oxygen ions conductivity in such materials. The optimum t value was found to be around 0.96 due to balance between SFV and t in order to obtain maximum ionic conductivity [16]. The crystallographic analysis shows that the tolerance factor for pure barium zirconate is very close to unity, thus its cubic structure described by the space group of $Pm\bar{3}m$ is stable. Fig. 1 shows the changes of tolerance factors caused by the addition of strontium to the prepared solid solutions. All the structural factors were also calculated for $(Ba_{1−x}Sr_x)ZrO_3$, BS-Z, series as a reference. In each sample series a decrease of t value is observed regardless of the kind of the B-site dopant, yet the minimum t value is still over 0.97. For such value changes of the perovskite structure, e.g. transformation into the lower-symmetry lattice, are usually not observed. Such small changes can be the effect of mutual compensation of ionic radii changes—the smaller Sr^{2+} ($r = 132$ pm) for the larger Ba^{2+} ($r = 149$ pm) but the larger Y^{3+} ($r = 104$ pm) or La^{3+} ($r = 117$ pm) for the smaller Zr^{4+} ($r = 86$ pm). It is also shown that a substitution of the bigger lanthanum ions, when compared to the yttrium ones, for the zirconium ions caused larger changes of the tolerance factor. The specific free volume determines a possibility of oxygen ions and, indirectly, protons migration and thus their conductivity in perovskite materials. It was shown that good oxygen conductors were the perovskites with SFV values higher than 0.4 [16–18].

The substitution of yttrium or lanthanum for zirconium in BaZrO$_3$ structure causes the increase of the specific free volume when compared to pure BaZrO$_3$, Fig. 2. Similar results are shown
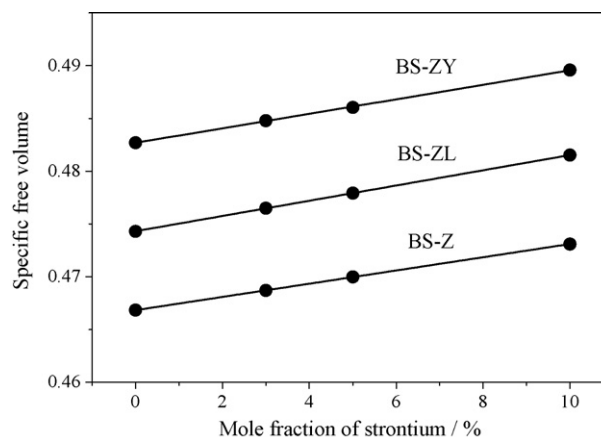

Fig. 2. Compositional dependence of the specific free volume for $(Ba_{1−x}Sr_x)(Zr_{0.9}M_{0.1})O_3$, M = Y, La, solid solutions.
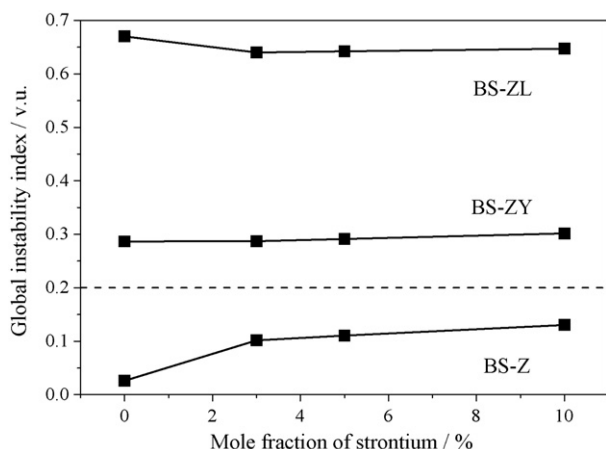
Fig. 3. Compositional dependence of the global instability index for $(Ba_{1-x}Sr_x)(Zr_{0.9}M_{0.1})O_3$, M = Y, La, solid solutions.

Fig. 4. Compositional dependence of the lattice parameters of the $(Ba_{1-x}Sr_x)(Zr_{0.9}M_{0.1})O_3$, M = Y, La, solid solutions.

when the strontium ions are substituted for the barium ones—the SFV values increase. A smaller ionic radius of strontium when compared to that of barium and the presence of oxygen vacancies are the reasons of SVF increase. The calculated changes of the SVF values suggest that the presence of strontium in the respective $BaZrO_3$ solid solutions should improve oxygen ions and, indirectly, protons conductivity in hydrogen or/and steam containing atmospheres. Experimental values of lattice constants of different solid solutions were used in the calculations.

The tolerance factor and specific free volume are based on geometric relations in the perovskite structure assuming that it is highly ionized and the ion shapes can be described as rigidly spherical. The overall structure stability is determined also by comparing the calculated bond valence sums with the ideal formal valences. This quantity is referred to as the global instability index, GII [19]. The GII value is typically <0.1 valence units (v.u.) for unstrained structures and as large as 0.2 v.u. in the structure with lattice induced strains. According to [20], the GII value of about 0.20 v.u. has been found critical for several structures typically found to be unstable.

Fig. 3 shows composition dependences of the global instability index for the $(Ba_{1-x}Sr_x)ZrO_3$, $(Ba_{1-x}Sr_x)(Zr_{0.9}Y_{0.1})O_3$ and $(Ba_{1-x}Sr_x)(Zr_{0.9}La_{0.1})O_3$ series. The GII value for pure $BaZrO_3$ as low as 0.026 confirms stability of its structure. The substitution of strontium for barium in the solid solution generally caused the increase of the GII value but it is less than 0.2 v.u., even for the maximum mole fraction of strontium. The global instability index value for $Ba(Zr_{0.9}Y_{0.1})O_3$, equal to 0.287, is unexpectedly high. It means that such a compound should be structurally unstable which is in contradiction to several literature data [21,22] and the present work. A further increase of strontium fraction in BS-ZY solid solutions causes the increase of GII values, similarly as in the BS-Z series. The global instability index for $Ba(Zr_{0.9}La_{0.1})O_3$ is as high as 0.670 and the substitution of strontium for barium increases it additionally. It is worth noticing that the presence of a small amount of Sr in the BS-ZL solid solution led to a transition decrease of GII value. To explain such a discrepancy the stabilization effect of oxygen vacancies should be also taken into consideration.

The applied method of preparation, decomposition of the organo-metallic precursors followed by milling, leads to obtaining good sinterable powders. Generally, all samples sintered at 1600 °C for 4 h achieved relative density exceeding 96% of theoretical density. The X-ray diffraction analysis reveals that all sintered samples are monophase and only the cubic $BaZrO_3$ phase is detected. The linear compositional dependence of the lattice
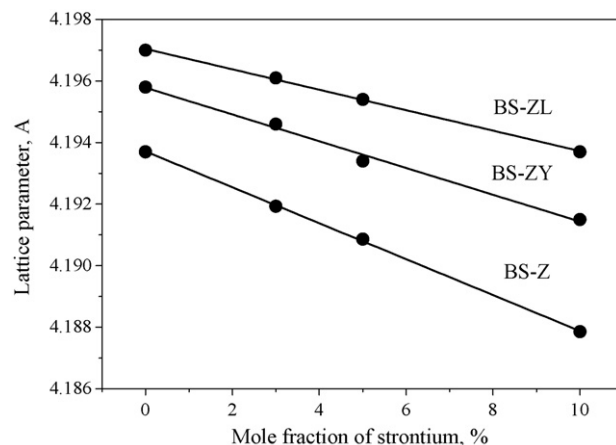
parameters complied with Vegard's rule confirms the formation of the respective solid solutions, Fig. 4. As it might be expected, according to the respective ionic radii, the substitution of yttrium or lanthanum for zirconium leads to the increase of the lattice parameters whereas the substitution of strontium for barium causes their decrease.

The oxygen transference numbers were measured using a galvanic cell (1) in which the B-ZY and B05S-ZY were used as solid electrolytes and Cu, Cu_2O and Ni, NiO mixtures as reversible electrodes [15]. The temperature dependences of the measured emf values for both samples are linear. The emf values were compared with the respective emf values (E_t), measured with the cell (1) containing 13CSZ. The calculated values of the oxygen transference numbers for both samples are over 0.98, what indicates that the oxygen ion conduction may be predominant at low oxygen partial pressure in dry atmosphere. On the other hand, at higher oxygen partial pressure, some increase of total electrical conductivity in B05S-ZY sample is observed, Fig. 5. Two different pO_2 regions can be distinguished, which corresponded to a different conduction mechanism. At a lower oxygen partial pressure, the total electrical conductivity is stable whereas at the oxygen partial pressure above 10^{-5} atm, the considerable increase of the total electrical conductivity is observed. This effect can be attributed to electronic conductivity caused by the formation of electronic holes via the
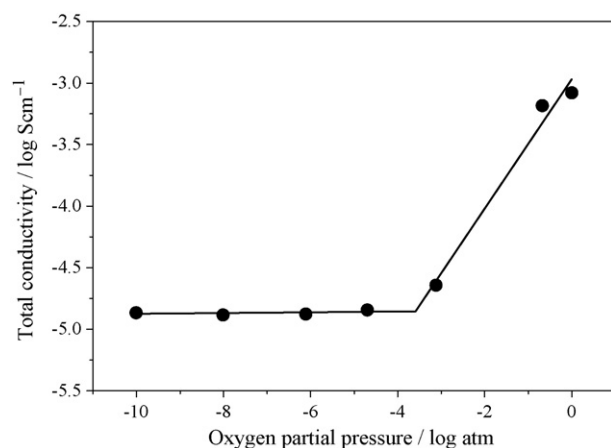

Fig. 5. Dependence of the total electrical conductivity on oxygen partial pressure for B05S-YZ sample at 600 °C.
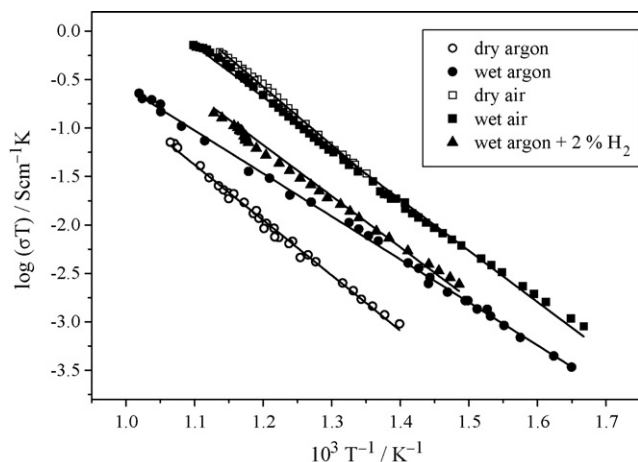
Fig. 6. Arrhenius plots for B05S-YZ sample in different atmospheres.

Fig. 8. Compositional dependence of the total conductivity of $(Ba_{1-x}Sr_x)(Zr_{0.9}Y_{0.1})O_3$ sample series. Measurements at 600 °C in different atmospheres.

following reaction:

$$V_O^{\bullet\bullet} + \frac{1}{2}O_2 \rightarrow O_o^x + 2h^{\bullet} \tag{3}$$

This result is in good agreement with the results of our previous investigations on the $(Ba_{1-x}Ca_x)(Zr_{0.9}Y_{0.1})O_3$ and $(Ba_{1-x}Ca_x)(Zr_{0.9}La_{0.1})O_3$ systems [12] and other literature data [23,24].

The temperature dependences of the total conductivity measured in different atmospheres for all samples are linear in Arrhenius coordinates. Fig. 6 shows demonstration dependences, measured for the sample $(Ba_{0.95}Sr_{0.05})(Zr_{0.9}Y_{0.1})O_3$ in different atmospheres, whereas Fig. 7 reveals the ones for all the samples measured in wet argon. In general, the solid solutions involving $(Ba_{1-x}Sr_x)(Zr_{0.9}Y_{0.1})O_3$ exhibit the higher total conductivity than the $(Ba_{1-x}Sr_x)(Zr_{0.9}La_{0.1})O_3$ samples, regardless of the atmosphere. Among these, the solid solution of barium zirconate with 5 mol.% of strontium shows the highest total conductivity. The compositional changes of the total conductivity measured at 600 °C for both sample series are shown in Figs. 8 and 9. The partial substitution of strontium for barium in both investigated series causes the increase of total conductivity but such changes are limited; the barium zirconate solid solutions with 10 mol.% of strontium showed the total conductivity close to $Ba(Zr_{0.9}Y_{0.1})O_3$ and $Ba(Zr_{0.9}La_{0.1})O_3$, respectively. It can also be seen that the lowest total conductivities for all samples were measured in dry argon. The presence of 2 vol.% of hydrogen in dry argon increased the total conduc-
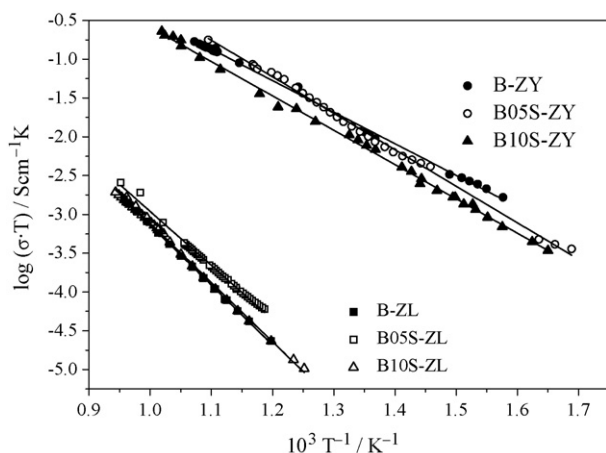
tivity, irrespectively of the chemical composition of the samples which confirmed the ability of the investigated materials to proton conduction. An increase of the steam partial pressure in wet argon, which also means an increase of the oxygen partial pressure due to the chemical reaction of water decomposition, caused an increase of the total conductivity. This effect can be related to the model of proton transport in the perovskite structure which assumed the presence of oxygen vacancy and their mobility that was smaller than protonic defects [25,26]. A further increase of the total conductivity measured in atmospheres with the higher partial pressure of oxygen (dry air) and steam (wet air) corroborates these statements. On the other hand, an increase of the oxygen partial pressure causes a formation of electron which was previously confirmed.

The described changes of the total conductivity result from the respective values of activation energies of conductivity, E_a, and pre-exponential factors, σ_0. Figs. 10 and 11 present compositional changes of the E_a determined from the Arrhenius plots. All samples show the highest activation energy of conductivity in dry argon regardless of their chemical composition and the increase of the steam and/or oxygen partial pressure cause decrease of the E_a values.

The described effects can be attributed to the local changes in the cubic perovskite structure improving oxide and proton ionic conductivity in hydrogen or water vapour containing atmosphere.

Fig. 7. Arrhenius plots for the both sample series. Measurements in wet argon.

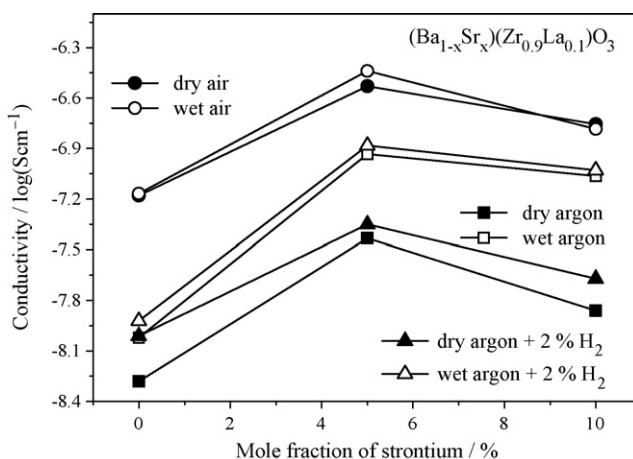**Fig. 9.** Compositional dependence of the total conductivity of $(Ba_{1-x}Sr_x)(Zr_{0.9}La_{0.1})O_3$ sample series. Measurements at 600 °C in different atmospheres.
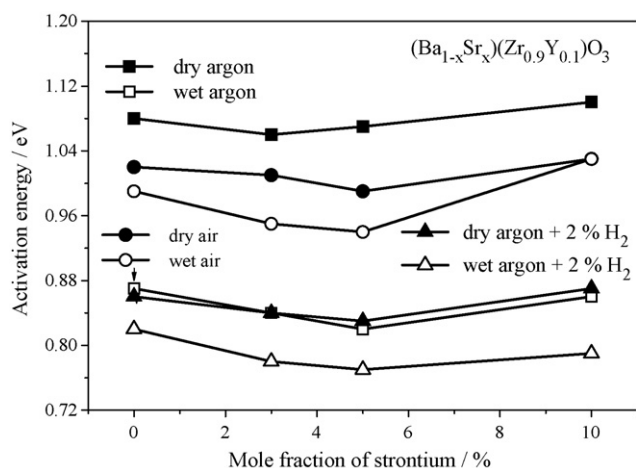
Fig. 10. Compositional dependence of the activation energy of conductivity for $(Ba_{1-x}Sr_x)(Zr_{0.9}Y_{0.1})O_3$ sample series.

According to the model of proton migration in perovskites, it was previously confirmed that the presence of proton in the perovskite structure induces strong but temporary interaction between proton and the oxygens in the ZrO_6 octahedra [22,25,27]. Such a structure is stable and not favourable towards proton migration unless the trivalent cations are substituted for the zirconium ones. In such a case an oxygen vacancy is formed and local distortion of the crystal lattice makes a formation of located O–H bond possible. This relatively strong bond can be easily moved from one oxygen to another by the hopping mechanism. The effect of the dynamically changed O–H bonds, responsible for high mobility of protons, is possible because of a local "softening" of the crystal structure in the vicinity of oxygen vacancy [7,8]. Difference between the ionic radii of barium and dopant is responsible for magnitude of such "softening" but, on the other hand, it is also a source of some structural stresses. The compositional changes of the total conductivity showed in the present paper (Figs. 8 and 9) suggest that a substitution of a smaller cation (Sr) for a bigger one (Ba) in the A-site intensifies such structural changes.

The observed relations between the total conductivity or the activation energy and chemical composition of the samples show real connections between electrical properties and substitution both in A- and B-site in perovskite structure. The improvement of

the ionic conductivity is essentially stronger when yttrium is substituted for zirconium. Based on structural relations (Figs. 1–3) it can be stated that specific free volume has the strongest influence on the ionic conductivity. It is also worth noticing that the lattice parameter of the best conductive sample, B05S-ZY, is very similar to the pure $BaZrO_3$ one that is the most stable structure. It suggests that the substitution of strontium for barium can compensate the lattice stresses caused by difference between the zirconium and yttrium or lanthanum ionic radii.

4. Summary

The decomposition of the organo-metallic precursors with EDTA followed by milling leads to the powders of the barium zirconate solid solutions showing good sinterability. The substitution of strontium for barium as well as of yttrium or lanthanum for zirconium influences structural properties of the resulting solid solutions. It was found that the introduction of strontium into solid solution, regardless the cation substituted in the B-site, causes a decrease of the tolerance factor as well as an increase of specific free volume and global instability index. It means, that the structures of respective solid solutions become a little less stable but of better conductivity. Electrical conductivity measurements performed in atmospheres containing argon, air, hydrogen and/or water vapour show that the conductivity depends both on a chemical composition of the samples and the atmosphere. In general, the electrical conductivity of respective solid solution is higher in wet atmospheres which contained oxygen, being in accordance with the model of a proton transport in the perovskite structure which assumed the presence of the oxygen vacancies. On the other hand, the solid solution containing 5 mol.% of strontium showed the highest conductivity and the lowest activation energy of conductivity regardless of the atmospheres. The relations between the total conductivity or the activation energy and structural properties of the solid solutions suggest that a substitution of a smaller cation (Sr) for a bigger one (Ba) in the A-site intensifies structural changes necessary for proton conduction.

References

[1] T. Schober, Solid State Ionics 162/163 (2003) 277–281.
[2] S.M. Haile, Mater. Today 6 (2003) 24–29.
[3] Ch. Kokkofitis, M. Ouzounidou, A. Skodra, M. Stoukides, Solid State Ionics 178 (2008) 475–480.
[4] P. Stuart, T. Unno, J.A. Kilner, J.S. Skinner, Solid State Ionics 179 (2008) 1120–1124.
[5] K. Katahira, Y. Kohchi, T. Shimura, H. Iwahara, Solid State Ionics 138 (2000) 91–98.
[6] S.V. Bhide, A.V. Virkar, J. Electrochem. Soc. 146 (1999) 2038–2044.
[7] T. Norby, Solid State Ionics 125 (1999) 1–11.
[8] E. Matsushita, T. Sasaki, Solid State Ionics 125 (2000) 31–37.
[9] M.S. Islam, Solid State Ionics 154/155 (2002) 75–85.
[10] M.S. Islam, R.A. Davies, J.D. Gale, Solid State Ionics 126 (1999) 323–335.
[11] S. Imashuku, T. Uda, Y. Nose, K. Kishida, H. Inui, Y. Awakura, J. Electrochem. Soc. 155 (2008) B581–B586.
[12] M. Dudek, M. Bućko, J. Solid State Electrochem., in press, doi:10.1007/s10008-008-0706-0.
[13] M.W. Lufaso, P.M. Woodward, Acta Cryst. B57 (2001) 725–738.
[14] G. Charette, S.N. Flengas, J. Electrochem. Soc. 115 (1968) 796–804.
[15] K. Kiukola, C. Wagner, J. Electrochem. Soc. 104 (1957) 379–387.
[16] H. Hayashi, H. Inaba, M. Matsuyama, N.G. Lan, M. Dokiya, H. Tagawa, Solid State Ionics 122 (1999) 1–15.
[17] A. Mantihram, J. Kuo, J.B. Goodenough, Solid State Ionics 62 (1993) 225–234.
[18] R. Cook, A. Sammells, Solid State Ionics 45 (1991) 311–321.
[19] A. Salinas-Sanchez, J.L. Garcia-Munoz, J. Rodriguez-Carvajal, R. Saez-Puche, J. Solid State Chem. 100 (1992) 201–211.
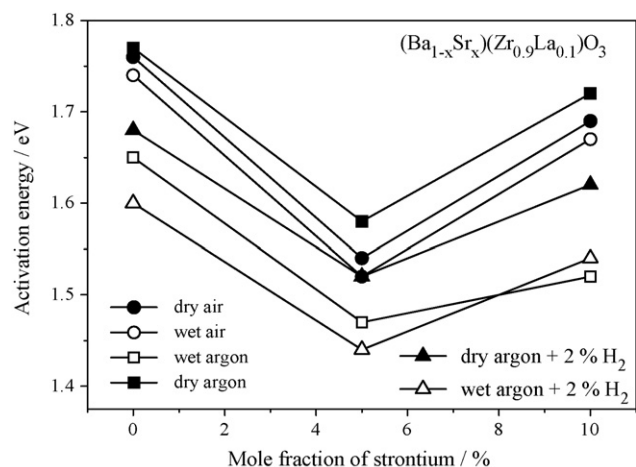

Fig. 11. Compositional dependence of the activation energy of conductivity for $(Ba_{1-x}Sr_x)(Zr_{0.9}La_{0.1})O_3$ sample series.

[20] I.D. Brown, Acta Cryst. B48 (1992) 553–572.
[21] R.C.T. Slade, S.D. Flint, N. Singh, Solid State Ionics 82 (1995) 135–141.
[22] K.D. Kreuer, Solid State Ionics 125 (1999) 285–302.
[23] T. Schober, H.G. Bohn, Solid State Ionics 127 (2000) 351–360.
[24] N. Kurita, N. Fukatsu, K. Ito, T. Ohashi, J. Electrochem. Soc. 142 (1995) 1552–1559.

[25] A. Nowick, Y. Du, K. Liang, Solid State Ionics 125 (1999) 303–311.
[26] N. Sata, H. Yugami, Y. Akiyama, H. Sone, H. Kitamura, T. Hattori, M. Ishigame, Solid State Ionics 125 (1999) 383–387.
[27] K.D. Kreuer, Solid State Ionics 136/137 (2000) 149–160.